doi:10.1093/jmcb/mjaa066
Published online December 19, 2020

Article

Ggps1 deficiency in the uterus results in dystocia by disrupting uterine contraction

Yong-Juan Sang[1,†], Qiang Wang[2,†], Feng Zheng[1], Yue Hua[1], Xin-Ying Wang[1], Jing-Zi Zhang[1], Kang Li[1], Hai-Quan Wang[1], Yue Zhao[1], Min-Sheng Zhu[1,*], Hai-Xiang Sun[1,*], and Chao-Jun Li[1,*]

[1] State Key Laboratory of Pharmaceutical Biotechnology, Center for Reproductive Medicine, Department of Obstetrics and Gynecology, Nanjing Drum Tower Hospital, The Affiliated Hospital of Nanjing University Medical School, Model Animal Research Center, Nanjing University, Nanjing 210093, China
[2] Department of Neurosurgery, Jingling Hospital, School of Medicine, Nanjing University, Nanjing 210002, China
[†] These authors contributed equally to this work.
[*] Correspondence to: Chao-Jun Li, E-mail: licj@nju.edu.cn; Hai-Xiang Sun, E-mail: stevensunz@163.com; Min-Sheng Zhu, E-mail: zhums@nicemice.cn

Edited by Jinsong Li

Dystocia is a serious problem for pregnant women, and it increases the cesarean section rate. Although uterine dysfunction has an unknown etiology, it is responsible for cesarean delivery and clinical dystocia, resulting in neonatal morbidity and mortality; thus, there is an urgent need for novel therapeutic agents. Previous studies indicated that statins, which inhibit the mevalonate (MVA) pathway of cholesterol synthesis, can reduce the incidence of preterm birth, but the safety of statins for pregnant women has not been thoroughly evaluated. Therefore, to unambiguously examine the function of the MVA pathway in pregnancy and delivery, we employed a genetic approach by using myometrial cell-specific deletion of *geranylgeranyl pyrophosphate synthase* (*Ggps1*) mice. We found that *Ggps1* deficiency in myometrial cells caused impaired uterine contractions, resulting in disrupted embryonic placing and dystocia. Studies of the underlying mechanism suggested that *Ggps1* is required for uterine contractions to ensure successful parturition by regulating RhoA prenylation to activate the RhoA/Rock2/p-MLC pathway. Our work indicates that perturbing the MVA pathway might result in problems during delivery for pregnant females, but modifying protein prenylation with supplementary farnesyl pyrophosphate or geranylgeranyl pyrophosphate might be a strategy to avoid side effects.

Keywords: uterine contraction, protein prenylation, dystocia, statin, RhoA

Introduction

Myometrial or uterine smooth muscle (USM) contraction and relaxation are fundamental behaviors of the uterus essential for normal reproduction in humans. In the nonpregnant state, USM generates peristalsis to facilitate the expulsion of menses (Kunz and Leyendecker, 2002; Bulletti et al., 2004). This peristalsis is also required for embryo implantation and pregnancy establishment. During pregnancy, USM contractile activity subsides to maintain pregnancy (Garfield and Maner, 2007; Aguilar and Mitchell, 2010). As pregnancy approaches full term, USM generates synchronized and coordinated contractions, leading to fetal delivery (Smith et al., 2015). Dysfunction in uterine contractility is a major cause of various obstetrical and gynecological disorders, such as dysmenorrhea, adenomyosis, miscarriage, preterm labor (PTL), and postpartum bleeding.

The mevalonate (MVA) pathway plays key roles in diverse physiological and pathological processes. Statins are inhibitors of 3-hydroxy-3-methylglutaryl-CoA reductase (HMGCR) in the MVA pathway (Moghadasian, 1999). Statins have been extensively used in the clinic as an effective treatment for hypercholesterolemia, but the strategies for applying these drugs appropriately in the clinic require more comprehensive research. Considering the incidence of hyperlipidemia and increased cholesterol levels during pregnancy, statins are a potential but controversial therapeutic option for pregnant women (Nasioudis et al., 2019). Additionally, previous studies have suggested that statins can exert anticontractile effects on

Received April 27, 2020. Revised August 28, 2020. Accepted September 18, 2020.

vascular smooth muscle cells and endometriotic stromal cells, as well as on mouse and human myometrial tissue (Mraiche et al., 2005; Perezguerrero et al., 2005; Nasu et al., 2009; Gonzalez et al., 2014), suggesting statins as potential therapeutics for the prevention of spontaneous PTL. In contrast, the use of statins increases the risk of female dystocia because of the anticontractile effects and disrupts fetal development, e.g. leading to limb defects (Mraiche et al., 2005; Ofori et al., 2007). Due to the side effects of statins, which have not been evaluated properly and comprehensively *in vivo*, it is controversial whether these drugs should be investigated in clinical trials to ameliorate plasma lipids or prevent human preterm birth (PTB).

MVA is converted to sterol and nonsterol isoprenoid, of which farnesyl pyrophosphate (FPP) and geranylgeranyl pyrophosphate (GGPP) are two major intermediates. Geranylgeranyl pyrophosphate synthase (Ggps1) is an important enzyme that catalyzes the synthesis of GGPP from FPP (Goldstein and Brown, 1990). Both FPP and GGPP contribute to protein prenylation by farnesyl transferase and geranylgeranyl transferase, respectively, by conjugating lipid anchors to target proteins, which are essential for their association with and activation at the plasma membrane (Schafer and Rine, 1992). Isoprenylation of GGPP is crucial for the activation of small GTPases, such as Rho, Rac, and Cdc42, which are associated with various cellular functions, including gene expression and actin cytoskeleton remodeling. The cross-bridging of the myofilaments actin and myosin is essential for contraction of the myometrium, which is facilitated by the phosphorylation of myosin light chain (MLC) (Word et al., 1993). The above-mentioned evidence supports the investigation of the role of the Ggps1-involved MVA pathway in physiological uterine contractions.

In the present study, we constructed a genetic mouse model in which *Ggps1* is knocked out in the myometrium though anti-Müllerian hormone type 2 receptor (*Amhr2*)-specific Cre recombinase; these mice were named *Ggps1* conditional knockout (*Ggps1* cKO) mice and are unable to produce GGPP for intermediate synthesis and geranylgeranylation. *Amhr2*-Cre also has high expression in granulosa cells and can be used to generate a granulosa cell-specific knockout mouse model (Arango et al., 2008). Unexpectedly, in this study, we found that the expression of *Ggps1* in granulosa cells was not essential for ovarian function. However, we found that *Ggps1* deficiency in myometrial cells caused impaired uterine contractions, resulting in disrupted embryonic placing and dystocia.

Results

Ggps1 is expressed in oocytes and granulosa cells of the ovary and uterus

We checked the expression of *Ggps1* in the female reproductive system with an immunohistochemical (IHC) staining method. We found that *Ggps1* was expressed in oocytes and granulosa cells at different developmental stages (Figure 1A). Furthermore, *Ggps1* was abundantly expressed in the uterus, mainly in the endothelium and smooth muscle layers (Figure 1D). Our previous work revealed that *Ggps1* is critical in oocytes for primary–secondary follicle transition through its effects on oocyte–granulosa cell communication (Jiang et al., 2017). Herein, we aimed to ascertain the role of *Ggps1* in granulosa cells by deleting *Ggps1*. To accomplish this, *Ggps1*-floxed mice (*Ggps1*$^{fl/fl}$) were crossed with *Amhr2-Cre* mice, in which *Amhr2*-Cre is expressed in Müllerian duct-derived cells (e.g. granulosa cells and smooth muscle cells of the uterus and oviduct); thus, this cross would delete *Ggps1* conditionally in these cells. The analyses of mRNA and protein levels suggested that *Ggps1* expression was largely lost in the ovary (Figure 1B and C; Supplementary Figure S1A) and uterus (Figure 1E and F; Supplementary Figure S1B). IHC staining also showed that *Ggps1* was successfully knocked out in granulosa cells of follicles (Figure 1A) and the myometrium (Figure 1D). Thus, we had created a model for exploring the function of *Ggps1* in controlling protein prenylation during female reproduction.

Mice with Ggps1 deletion in granulosa cells and the myometrium show normal follicle and uterus development

Although *Amhr2*-Cre is expressed in granulosa cells and smooth muscle cells of the uterus, to our surprise, no issues with follicle or uterus development were found in *Ggps1* cKO mice. There were no changes in body weight or in the weight or morphology of the uterus (Supplementary Figure S2A; Figure 2A and B) or ovary (Figure 2C and D). We counted the number of follicles at different stages and found that the numbers of primordial, primary, and secondary follicles (Figure 2E–G) in 6-week-old mice were not different between *Ggps1* cKO and control mice. The number of fertilized eggs collected from the oviducts was also not different between *Ggps1* cKO and control mice (Figure 2H). All the data indicated that *Ggps1* deficiency in granulosa cells of follicles and the myometrium did not affect follicle or uterus development.

Ggps1 deletion results in oviduct and embryo implantation abnormalities in the uterus

As stated above, no gross morphological or histological abnormalities were observed in the ovary or uterus. However, another Müllerian duct-derived organ, the oviduct, was found to be abnormal in *Ggps1* cKO mice. The oviducts in *Ggps1* cKO mice were smaller and shorter (Figure 3A–C), as well as lighter, than those in the control mice (Figure 3D). Hematoxylin and eosin (H&E) staining of mouse oviducts showed that the oviduct wall of *Ggps1* cKO mice was thinner than that of control mice (Figure 3E). Normally, oocytes are released from the ovary, collected by the oviduct, and fertilized inside the ampulla, after which peristaltic contractions and cilia of the epithelial folds move the fertilized eggs into the uterus, where they implant in the endometrium. When we examined

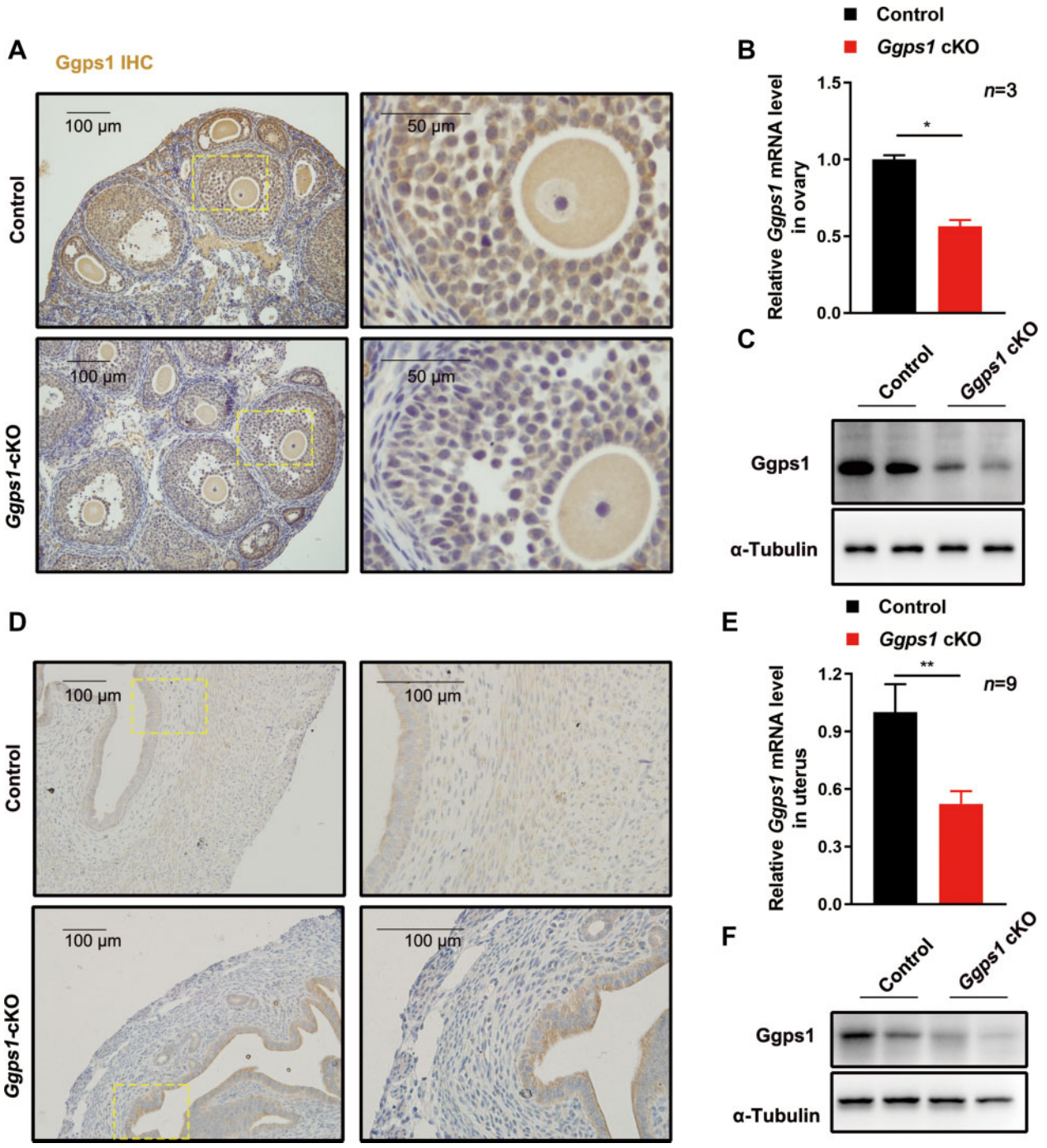

Figure 1 Mice with *Ggps1* deletion in ovarian granulosa cells and myometrial cells are generated using *Amhr2-Cre* mice. (**A**) IHC staining of Ggps1 in the ovaries of 3-week-old control and *Ggps1* cKO mice. (**B**) Quantitative real-time PCR (qPCR) analysis of *Ggps1* in ovaries of 3-week-old control and *Ggps1* cKO mice. (**C**) Western blot analysis of Ggps1 in ovaries of 3-week-old control and *Ggps1* cKO mice. α-Tubulin served as an internal control. (**D**) IHC staining of Ggps1 in the uterus of 3-week-old control and *Ggps1* cKO mice. (**E**) qPCR analysis of *Ggps1* in the uterus of 3-week-old control and *Ggps1* cKO mice. (**F**) Western blot analysis of Ggps1 in the uterus of 3-week-old control and *Ggps1* cKO mice. α-Tubulin served as an internal control. Data are presented as mean ± SEM. $*P < 0.05$, $**P < 0.01$, unpaired two-tailed Student's *t*-test.

embryonic implantation in the uterus at 4.5 days post coitum (dpc), we found that although the number of implanted embryos was not affected (Figure 3F), the embryonic spacing was not even in *Ggps1* cKO mice (Figure 3G). Therefore, *Ggps1* is critical for oviduct development and ordered embryonic implantation.

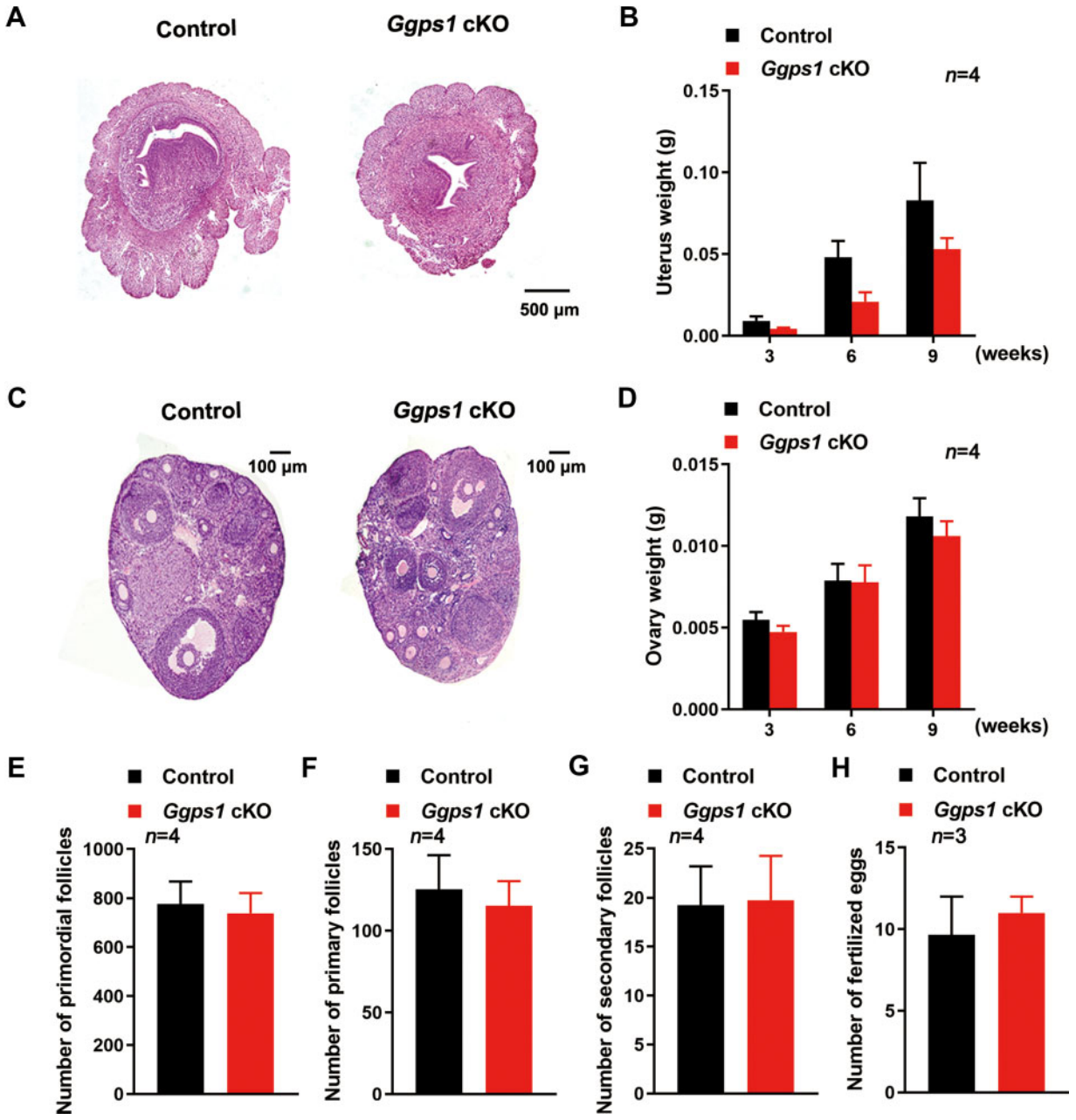

Figure 2 Mice with *Ggps1* deletion in granulosa cells and the myometrium show normal follicle and uterus development. (**A**) Representative photographs of H&E staining of the uterus from 6-week-old control and *Ggps1* cKO mice. (**B**) Female mice with *Ggps1* deletion in myometrial cells showed normal uterus development compared with control mice. The uterus weight in the control and *Ggps1* cKO groups is shown at 3, 6, and 9 weeks. (**C**) Representative photographs of H&E staining of ovaries from 3-week-old control and *Ggps1* cKO mice. (**D**) Female mice with *Ggps1* deletion in ovarian granulosa cells showed normal ovary development compared with control mice. The ovary weight in the control and *Ggps1* cKO groups is shown at 3, 6, and 9 weeks. (**E**–**G**) *Ggps1* deletion in granulosa cells and myometrial cells did not affect follicle development. Quantification of the different types of follicles, including primordial (**E**), primary (**F**), and secondary follicles (**G**), in ovaries from control and *Ggps1* cKO mice. The number of follicles per ovary was quantified. (**H**) Female mice with *Ggps1* deletion in ovarian granulosa cells showed normal fertilization during natural mating. Control and *Ggps1* cKO mice were mated with fertile wild-type males. Data are presented as mean ± SEM. $*P < 0.05$, $**P < 0.01$, unpaired two-tailed Student's *t*-test.

Ggps1 deletion results in subfertility and dystocia

Abnormal embryonic implantation can result in pregnancy loss; thus, we examined fertility by mating female *Ggps1* cKO mice with fertile 8-week *C57BL/6J* males. The results showed that female mice with *Ggps1* deletion were subfertile compared with control female mice (Figure 4A). Surprisingly, although parturition was invariably initiated at term (~19.5 days), 75% of pregnant *Ggps1* cKO females experienced

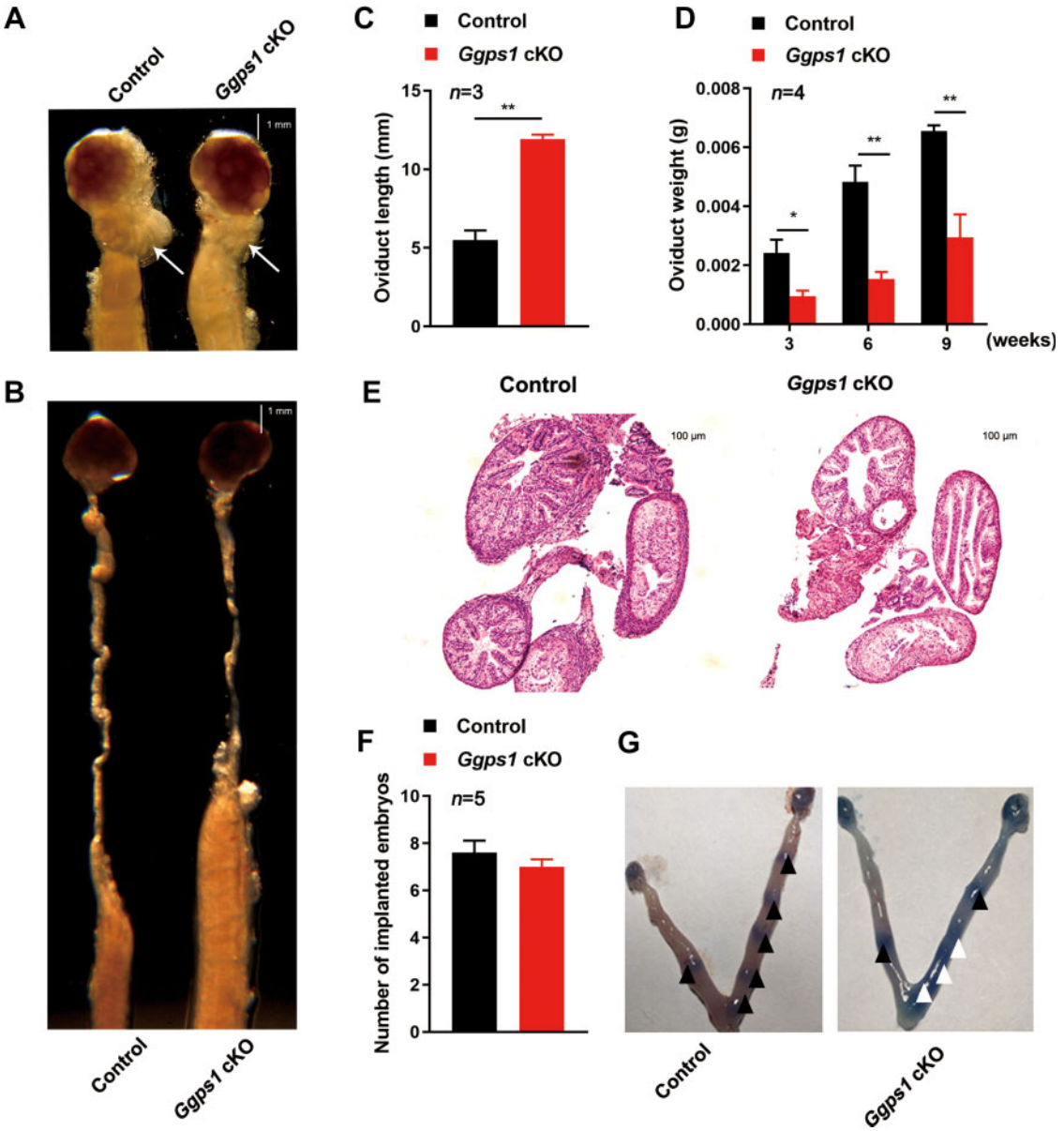

Figure 3 *Ggps1* deletion results in oviduct and embryo implantation abnormalities in the uterus. (**A**) Representative images of oviducts in 6-week-old mice were captured using a light microscope. The white arrowheads indicate oviducts. (**B** and **C**) *Ggps1* cKO oviducts were shorter than control oviducts at 6 weeks. (**D**) *Ggps1* cKO mice had lighter oviducts than control mice at the indicated time points, including 3, 6, and 9 weeks. (**E**) H&E staining of oviducts indicated that *Ggps1* cKO oviducts were thinner than control oviducts. (**F** and **G**) *Ggps1* cKO mice showed normal embryo implantation but disrupted embryo spacing at 4.5 dpc. Six-week-old female mice were mated with fertile wild-type males and then injected with Evans blue to visualize the embryo implantation sites. Data are presented as mean ± SEM. $*P < 0.05$, $**P < 0.01$, unpaired two-tailed Student's *t*-test.

arrested or prolonged parturition with embryo retention in the uterus or birth canal or delivery of dead pups, while the control mice did not display any dystocia (Figure 4B and C). Since the corpora lutea derived from granulosa cells of ovulated follicles and the endometrium synthesizes and secretes progesterone to promote successful embryo implantation and reduces progesterone release to initiate parturition, we examined the levels of progesterone in pregnant mice at 18.5 dpc. However, progesterone levels were similar between *Ggps1* cKO and control (Figure 4D). Relaxin, another hormone, is secreted into circulation during pregnancy and influences pubic symphysis relaxation and parturition, so we checked the plasma level of relaxin. However, the levels of relaxin were also not different (Figure 4E). Thus, there is potentially a nonendocrine reason for dystocia after *Ggps1* deletion.

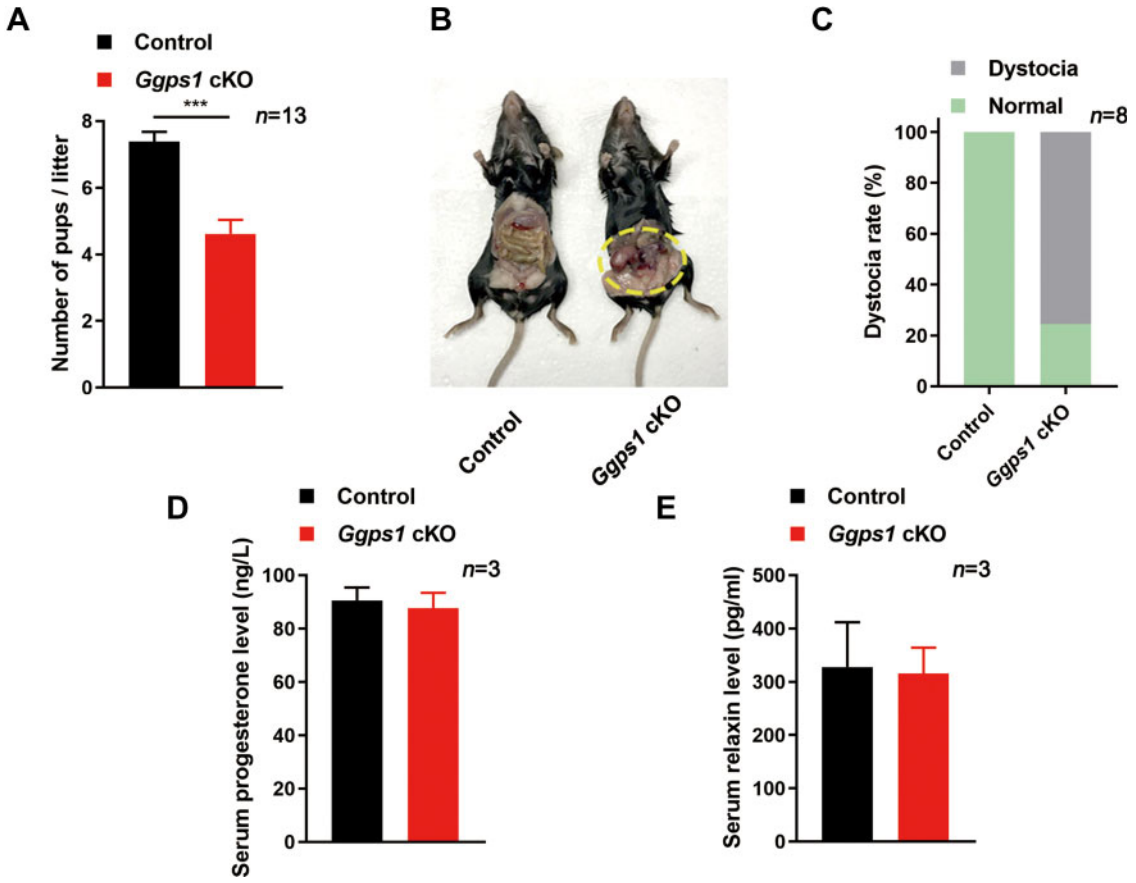

Figure 4 *Ggps1* deletion results in subfertility and dystocia. (**A**) Female mice with *Ggps1* deletion showed decreased fertility. Number of pups born to *Ggps1* cKO females compared with control females (Student's *t*-test). (**B**) Representative images of control and *Ggps1* cKO females at 20 dpc that gave birth to live pups. Circled area, uterus containing fetuses. (**C**) *Ggps1* cKO mice showed significantly increased dystocia. Fetuses that remained in utero were quantified at 20 dpc or 24 h after giving birth. (**D** and **E**) Serum progesterone and relaxin levels were comparable in control and *Ggps1* cKO pregnant mice at 18.5 dpc. Data are presented as mean ± SEM. $*P < 0.05$, $**P < 0.01$, unpaired two-tailed Student's *t*-test.

Ggps1 deficiency leads to defects in the RhoA/Rock2/p-MLC pathway by disrupting RhoA prenylation and causes impaired uterine contractions

Under physiological circumstances, the uterus is dormant during pregnancy to avoid PTB but undergoes a transformation to active contractions when expulsion of the fetus becomes necessary. *Amhr2*-Cre was confirmed to be specifically expressed in the myometrium (Supplementary Figure S3A), indicating that uterine contraction might be affected by *Ggps1* loss. Thus, we checked the contractile ability of the uterus after *Ggps1* knockout. We isolated uterine muscle strips from adult nonpregnant mice and found that the spontaneous contraction rate and amplitude in *Ggps1* cKO mice were irregular and lower, while the control mice showed regular and phasic contractions (Figure 5A). Moreover, the maximal contractile force in *Ggps1* cKO mice was largely decreased according to the response of the strips to KCl treatment (Figure 5B and C). The intrinsic reason for the disruption of uterine contractility was the marked inhibition of the phosphorylation of MLCs after *Ggps1* deletion in the myometrium (Figure 5D). The Rho/Rho-associated protein kinase (Rock) pathway is associated with smooth muscle contraction. As expected, we found that the membrane association of RhoA significantly decreased after *Ggps1* deletion in the myometrium (Figure 5E), and the expression of Rock2, the downstream target of Rho, was also decreased (Figure 5F). Thus, *Ggps1* deletion disrupts the RhoA/Rock2/p-MLC pathway by affecting protein prenylation and thus appropriate RhoA membrane localization, causing uterine contraction and parturition problems. Furthermore, we tried to determine the specific role of *Ggps1* in the myometrium by constructing a tamoxifen-induced *Ggps1* knockout mouse model but failed because of the negative effects of tamoxifen on uterine contraction (Supplementary Figure S3B and C).

Discussion

Our present study involving mice with *Ggps1* deletion in ovarian granulosa cells and the uterus reveals that *Ggps1* deficiency has no effect on ovarian functions, including follicle development and fertilization, which indicates that GGPP in

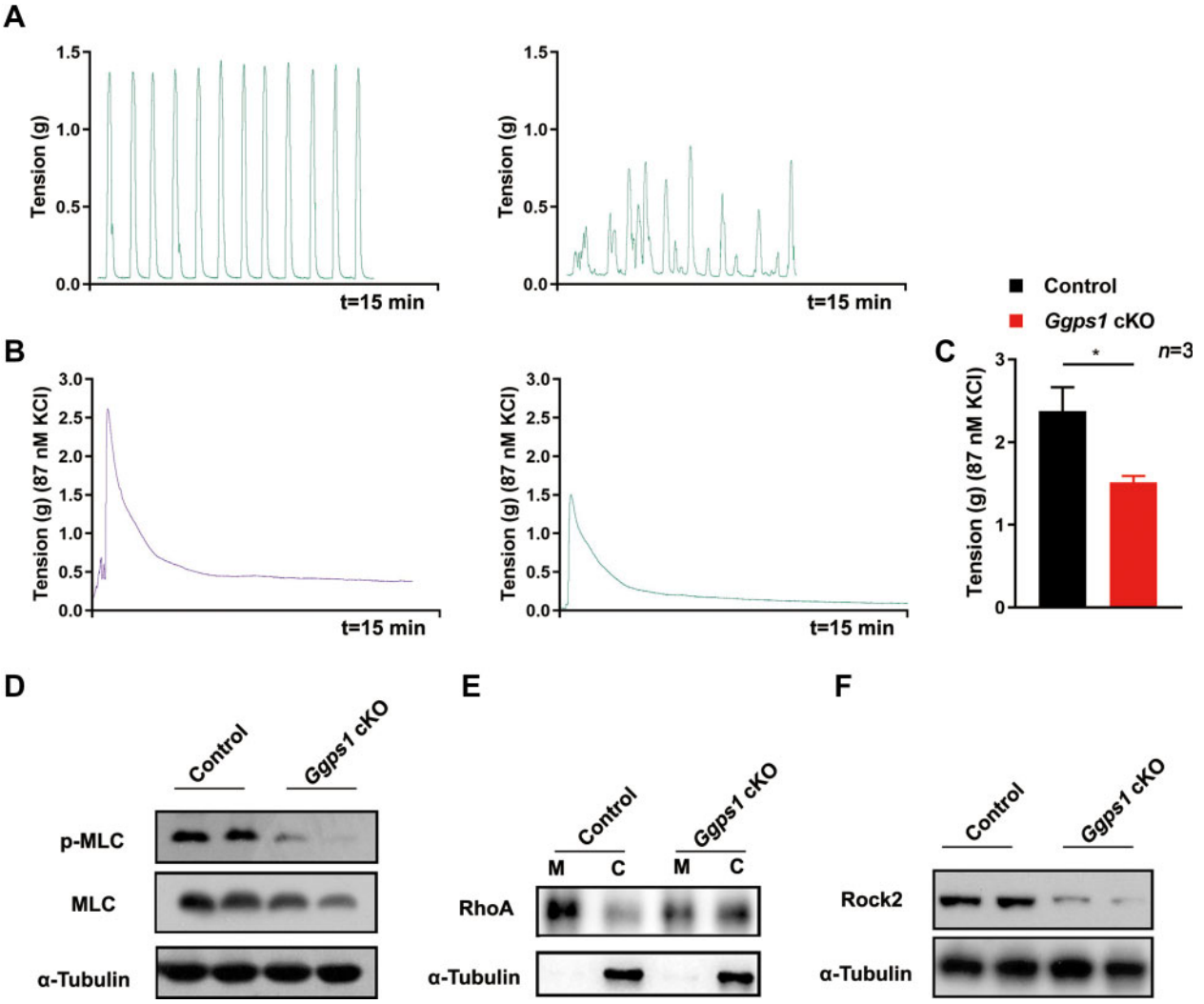

Figure 5 *Ggps1* deficiency impairs uterine contraction via the RhoA/Rock2/p-MLC pathway, which is responsible for dystocia. (**A**) *Ggps1* cKO mice displayed irregular contractions of lower amplitude compared with control mice. Left: control; right: *Ggps1* cKO. (**B** and **C**) The maximal contractile force of *Ggps1* cKO strips was largely decreased upon KCl treatment. Left: control; right: *Ggps1* cKO. (**D**) The levels of p-MLC were decreased in *Ggps1* cKO mice compared with control mice, as assessed by western blotting. α-Tubulin served as an internal control. (**E**) The membrane association of RhoA was reduced in the *Ggps1* cKO uterus, as determined by ultracentrifugation and western blot analysis. (**F**) The protein level of Rock2 was decreased in *Ggps1* cKO uterus compared with control, as assessed by western blotting. α-Tubulin served as an internal control. Data are presented as mean ± SEM. $*P < 0.05$, $**P < 0.01$, unpaired two-tailed Student's *t*-test.

granulosa cells is less important for ovarian function (Figure 6). In contrast, we found that *Ggps1* deficiency in the uterus causes dystocia and subfertility due to impaired myometrial contraction and disrupted embryo implantation (Figure 6). Additionally, *Ggps1* deletion resulted in a narrower and shorter oviduct. Here, we propose one possible mechanism wherein GGPP deficiency during uterine contraction underlies these phenotypes. We showed that GGPP depletion might disrupt uterine contraction by reducing RhoA through geranylgeranylation and inactivating the RhoA/Rock2/p-MLC pathway. Furthermore, these findings might provide useful information for the clinical application of statins.

The MVA biosynthesis pathway produces not only sterols but also nonsterols termed isoprenoids, such as FPP and GGPP (Goldstein and Brown, 1990; Casey, 1992; Supplementary Figure S4). As inhibitors of HMGCR in the MVA pathway, statins function within the upstream of the MVA pathway and inhibit both cholesterol synthesis and protein prenylation by direct inhibiting HMGCR (Leichner et al., 2011; Supplementary Figure S4). However, *Ggps1*, as an important branch point enzyme of the MVA pathway, determines the balance of protein prenylation by catalyzing the synthesis of GGPP from FPP, both of which are used for the prenylation of proteins with specific motifs at their C-terminal (Supplementary Figure S4). Even though previous studies in Hela cells show that mevastatin could induce slight induction of GGPS1 expression at mRNA level and upregulate RhoA expression transcriptionally and translationally, it is demonstrated that they are regulated by

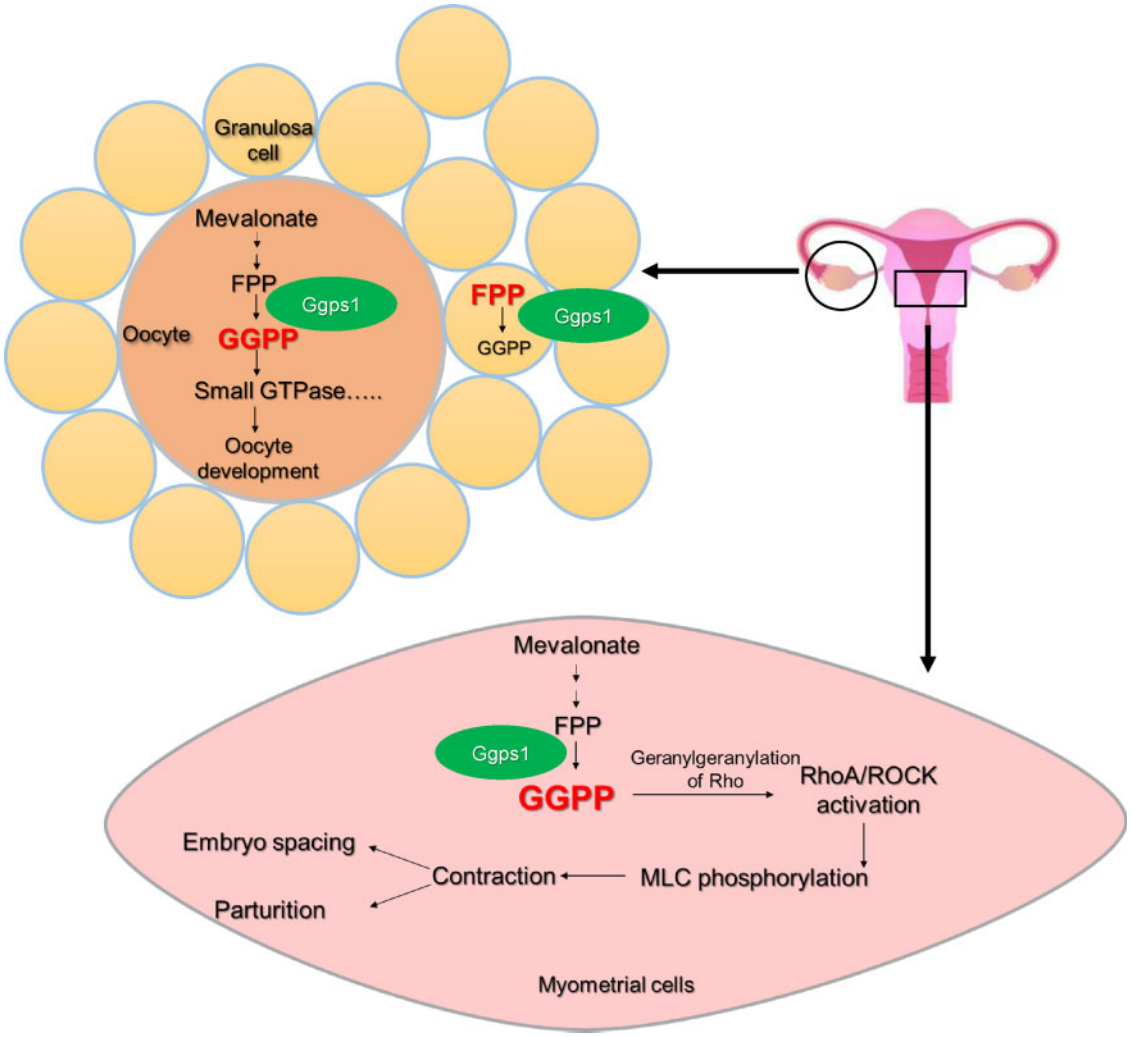

Figure 6 *Ggps1* deficiency in the uterus causes dystocia and subfertility, while *Ggps1* deletion in ovarian granulosa cells and the uterus has no effect on ovarian function.

negative feedback mechanism because of lack of GGPP (Gan et al., 2008). In inclusion, the level of GGPP but not Ggps1 can be affected by administration of statins. To understand the effects of statins on Ggps1 of mouse uterus and ovary *in vivo*, we tried injecting the adult female mice with simvastatin (20 μg/mice, 2 days) and checked the protein level of Ggps1. We found no changes of Ggps1 and protein prenylation in ovaries (Supplementary Figure S5A and B). However, the data showed that the protein level of Ggps1 was not affected whereas the protein prenylation of Rap1A was significantly decreased by short-time simvastatin administration in uterus (Supplementary Figure S5C and D). Therefore, protein prenylation responses to statin quickly and inhibited protein prenylation may be the critical reason for many side effects of statins. Statin treatment and *Ggps1* deletion produce similar effects in some cases.

Statins are widely considered potential treatments for certain features of cardiovascular disease and hepatic disorders (Yeh et al., 2016; Kamal et al., 2017). In terms of pregnant females, studies have revealed that statins can prevent fetal death in mouse models of recurrent miscarriage and antiphospholipid syndrome, as well as prevent abnormalities in the cortex of the fetal brain in a mouse model of PTB (Redecha et al., 2008, 2009; Pedroni et al., 2014). Even though RhoA/Rock pathway disruptions mediate the anticontraction effect of statin treatment, accumulating data indicate that statin use carries increasing risks during embryogenesis, such as deformed limbs and heart development failure due to unexpected pleiotropic effects (Bateman et al., 2015; Chen et al., 2018). Additionally, our work reveals that inhibition of the MVA pathway by *Ggps1* deletion causes dystocia due to disrupted uterine contraction. Based on data from our genetic knockout model, we propose that both the appropriate dosage and timing of statin administration are important in terms of ameliorating abnormal parturition.

Isoprenoids have been shown to play an important role in controlling metabolism and viability in both cancer and normal cells (Redecha et al., 2008; Moutinho et al., 2017). Other

studies revealed that simvastatin treatment can reduce the phosphorylation of MLC in myometrial cells, and GGPP supplementation abolished the anticontractile activity of simvastatin, suggesting that simvastatin exerts effects by inhibiting the geranylgeranylation of small GTPases (Boyle et al., 2018). Consistent with the results of a previous study, our data showed that Ggps1-produced GGPP is essential for the detergent-phase localization of RhoA and phosphorylation of MLC. This finding provides further evidence that the geranylgeranylation of small GTPases is responsible for myometrial contraction and successful parturition. Although the mechanisms responsible for the dystocia phenotype observed in our study have not been fully elucidated, they likely involve disrupted protein prenylation, which could be regarded as a novel therapeutic target. We, therefore, propose the potential use of statins to treat PTL or other complications in pregnant women, which could be ameliorated by supplementation with MVA and GGPP but not FPP and squalene.

Furthermore, considering the anticontractile effects in the myometrium, some clinical trials of statins to prevent PTL in human pregnancy are being planned. Although the treatment of PTL is likely to occur in the second or third trimester when organogenesis is mostly complete to avoid the risk of fetal limb defects in the first trimester (Petersen et al., 2008; Bateman et al., 2015), our previous work indicated that *Ggps1*-mediated protein geranylgeranylation plays an indispensable role in ventricular chamber maturation and acts as a stage-specific signal to regulate the establishment of cardiac cytoarchitecture during mid-gestation (Chen et al., 2018). In addition, our results revealed that *Ggps1* deletion has negative effects on fetal and maternal health due to dystocia. Thus, the risks will be realized if the treatment timing of statins during gestation is not appropriate, including being too late or too long.

It has been reported that *Ggps1* deletion in oocytes is associated with ovarian dysfunction. GGPP deficiency in oocytes induced by *DDX4*-Cre causes arrest of the primary–secondary follicle stage transition and premature ovarian failure (Jiang et al., 2017). Moreover, GGPP deficiency in growing oocytes causes female infertility with different phenotypes, indicating that GGPP affects ovarian function in a stage-specific manner. In addition to female fertility, GGPP is also important in male fertility regardless of the cell type. Sertoli cell-specific GGPP deficiency leads to spermatogonia loss (Wang et al., 2013) but not a Sertoli cell defect, and germ cell-specific GGPP deficiency also causes impaired spermatogenesis (Diao et al., 2016). In contrast, our study demonstrated that the granulosa cell-specific deletion of GGPP does not affect ovarian function, including follicle development and fertilization, suggesting that GGPP affects ovarian function in a cell-specific manner.

Recent studies reveal that *GGPS1* mutations cause muscular dystrophy/hearing loss/ovarian insufficiency syndrome (Foley et al., 2020), indicating *GGPS1* has a critical role in human. In their work, a total of 11 patients in 6 families carrying five different biallelic mutations in specific domains of *GGPS1* were identified. All post-pubertal females had primary ovarian insufficiency, which is consistent with our genetic work in animal model (Jiang et al., 2017; Foley et al., 2020), revealing that *Ggps1* is essential for early folliculogenesis and oocyte maturation in female fertility. Primary ovarian insufficiency might cause female infertility, that is possibly why no females with *Ggps1* mutations are found in human dystocia. Therefore, we speculate that *GGPS1* deficiency or SNP in somatic cells of uterus is responsible for some clinical human dystocia.

Amhr2-Cre mice are a useful tool to examine specific gene functions in granulosa cells during the progression from ovulation to luteinization and from folliculogenesis to luteinization (Jorgez et al., 2004; Haraguchi et al., 2019). In the cumulus–oocyte complex, oocytes cannot synthesize cholesterol and pyruvate; granulosa cells produce most of the cholesterol and pyruvate transferred to oocytes (Sugiura et al., 2005; Su et al., 2007). The metabolic flux of the MVA pathway involves cholesterol and subsequent sterols from FPP (Panda and Devi, 2004; Buhaescu and Izzedine, 2007). In addition, our previous work found that *Ggps1* deletion enhances glycolysis and pyruvate production in the liver (Liu et al., 2018). Therefore, *Ggps1* deletion would theoretically lead to FPP and pyruvate accumulation and have no effects on the synthesis of sterol hormones, which is why *Ggps1* is not essential in granulosa cells for ovarian function, confirming the differential requirements for the MVA pathway.

Overall, the results from genetic experimental models in the present study suggest that *Ggps1* has different roles in Müllerian duct-derived cells, including granulosa cells, the uterus, and oviducts. *Ggps1* deficiency has no effect on granulosa cells but disrupts uterine contraction and results in dystocia, suggesting that statins should be used carefully in pregnant women; modifying protein prenylation with supplementary FPP or GGPP is a potential strategy to avoid side effects.

Materials and methods

Animals

Mice were housed in groups in accordance with the regulations on mouse welfare and ethics of Nanjing University under conditions of 12-h dark–light cycles and free access to food and water. *C57BL/6J* mice and the double fluorescent *Cre* reporter line (Rosa26^{mTmG}) were purchased from GemPharmatech (China). Pregnant female mice were sacrificed under isoflurane inhalation followed by cervical dislocation at the indicated time points. All mouse experiments conformed to the NIH guidelines (Guide for the Care and Use of Laboratory Animals) and were carried out according to the protocol approved by the Animal Care and Use Committee of the Model Animal Research Center of Nanjing University, Nanjing, China.

Strategy and generation of cKO mice

Mice homozygous-floxed for *loxP* insertion in the *Ggps1* gene (*Ggps1*$^{fl/fl}$) were produced by GemPharmatech. *Amhr2-Cre* mice were generously donated by Dr Jia-Hao Sha (Nanjing Medical

University). We generated mice with cell-specific *Ggps1* deletion by crossing *Amhr2-Cre* transgenic mice with homozygous-floxed *Ggps1* mice to produce mice harboring *Ggps1* deletion in ovarian granulosa cells and derivatives of the Müllerian duct (i.e. oviduct, uterus, and cervix). The knockout lines (129) were backcrossed for a minimum of six generations to the *C57BL/6* background, which was the background of the *Ggps1-LoxP* mice. The littermates were used as controls. To perform lineage tracing of *Amhr2*-Cre in the uterus, mice were genotyped as $Amhr2^{cre/+}$; $Rosa^{mTmG/+/-}$ mice were obtained from matings of $Amhr2^{cre/+}$ males and $Rosa^{mTmG/+/+}$ females.

Fertility assay

To assess the fertility of these mice, 6-week-old female *Ggps1* cKO mice and control mice (wild-type or heterozygous) were mated with adult (8-week-old) *C57BL/6* males of known fertility. Female mice were checked daily in the morning for the presence of a seminal plug to confirm mating.

Fertilization

Adult 6-week-old *Ggps1* cKO and control females were mated with fertile *C57BL/6* males. The females were sacrificed at 0.5 dpc, and oviducts were flushed with MII solution to recover fertilized eggs. The morphology of these eggs was examined, and they were counted under a dissection microscope.

Morphology, histology, immunohistochemistry, and immunofluorescence

To characterize the general morphology of the *Ggps1* cKO female reproductive tract, mice were sacrificed at several developmental ages after natural mating, and ovarian, oviductal, and uterine function and morphology were evaluated. Fresh tissues were fixed overnight at 4°C in 4% PBS-buffered paraformaldehyde for immunohistochemistry or Bouin's fixative for H&E staining, dehydrated in ethanol, embedded in paraffin, and cut into 5 μm sections. For histological analysis, the sections were subjected to H&E staining according to a standard protocol. For IHC staining, paraffin sections were deparaffinized, rehydrated, and boiled in citrate buffer (pH 6.0) for antigen retrieval. Afterwards, paraffin sections were permeabilized, blocked, and incubated with the indicated primary antibodies at 4°C overnight. Subsequently, the sections were incubated with secondary antibodies for 1 h at room temperature. Ggps1 antibodies were used for immunohistochemistry (Thermo Fisher, 1:100). For immunofluorescence analysis, frozen sections were costained with DAPI.

Western blot analysis

Total protein was extracted from frozen uteri and ovaries using NP40 buffer/RIPA containing a protease/phosphatase inhibitor cocktail. The protein concentration in each sample was determined using the BCA Protein Assay (Bio-Rad Laboratories). The same amount of protein (50 μg) was separated by 8%–12% SDS–PAGE, and resolved proteins were transferred to polyvinylidene fluoride membranes (Invitrogen) by standard methods. Immunoblots were blocked with 5% milk solution and incubated overnight at 4°C with primary antibodies against Ggps1 (Thermo Fisher, 1:100), phosphorylated MLC (CST, 1:1000), MLC (CST, 1:1000), Rock2 (Upstate, 1:1000), RhoA (Santa Cruz, 1:200), and α-tubulin (Proteintech, 1:1000). Goat anti-rabbit or anti-mouse secondary antibodies (1:5000) were used. Immunodetection was carried out using an enhanced chemiluminescence (ECL) kit.

qPCR

The mouse uterus was carefully isolated and quickly cleaned by removing connective tissues. Subsequently, the samples were frozen and ground to homogeneity in liquid nitrogen. Total cellular RNA was isolated by using TRIzol (Invitrogen) as described in the manufacturer's instructions. cDNA was synthesized by PrimeScript™ RT Master Mix (TaKaRa) from 1 μg total RNA isolated with TRIzol reagent. The resulting cDNA was diluted 1:10 in sterile water, and 1-μl aliquots were used for qPCR. Primers for *Ggps1* and *18S* were synthesized by Integrated DNA Technology (Invitrogen). The resulting material was then used for independent qPCR, which was carried out on an Applied Biosystems HT7300 Sequence Detector. Each cDNA sample was run in triplicate, and target mRNA expression was normalized for RNA loading using 18S. The mRNA concentration in each sample was calculated relative to the vehicle control by using the $2^{-\triangle\triangle CT}$ analysis method.

Subcellular fractionation

To determine the membrane association of RhoA, subcellular fractionation was performed using ultracentrifugation (Blonder et al., 2006; Xu et al., 2015). Subcellular fractions were immunoprecipitated using the RhoA antibody and subsequently subjected to western blot analysis. Immunoprecipitation was performed according to a standard protocol.

Analysis of smooth muscle contractility

Six-week-old female mice were sacrificed by cervical dislocation. The uterine tissue was isolated and cut into 4 mm × 8 mm strips, which were mounted in a 37°C organ bath and tied with surgical silk to the hooks of a force transducer (MLT0202; ADInstruments) and length-adjusting micrometer. The force measurements were performed as described previously (He et al., 2008). The 8-mm-long uterine strips were placed in Ca^{2+}-free HEPES–Tyrode (H–T) buffer (pH 7.4) to wash out the lumen contents. The strips were transferred to the organ baths and equilibrated in oxygenated (95% O_2, 5% CO_2) H–T buffer for 15 min. H–T buffer containing 87 mM KCl was used to achieve membrane depolarization. KCl stimulation of contractions was followed by a 10-min recovery period in H–T buffer. The force per cross-sectional area was calculated from histologic measurements of the longitudinal muscle layer.

Statistical analysis

All data are presented as mean ± SEM after analysis using a two-tailed Student's test to compare two groups. A *P*-value <0.05 was considered to indicate statistical significance.

Supplementary material

Supplementary material is available at *Journal of Molecular Cell Biology* online.

Acknowledgements

The authors would like to thank Dr Jia-Hao Sha at Nanjing Medical University for donating *Amhr2-Cre* mice.

Funding

This work was supported by the National Natural Science Foundation of China (31530046) and the National Science and Technology Major Project (SQ2018YFC100242).

Conflict of interest: none declared.

References

Aguilar, H.N., and Mitchell, B.F. (2010). Physiological pathways and molecular mechanisms regulating uterine contractility. Hum. Reprod. Update *16*, 725–744.

Arango, N.A., Kobayashi, A., Wang, Y., et al. (2008). A mesenchymal perspective of Müllerian duct differentiation and regression in Amhr2-lacZ mice. Mol. Reprod. Dev. *75*, 1154–1162.

Bateman, B.T., Hernandez-Diaz, S., Fischer, M.A., et al. (2015). Statins and congenital malformations: cohort study. BMJ *350*, h1035.

Blonder, J., Chan, K.C., Issaq, H.J., et al. (2006). Identification of membrane proteins from mammalian cell/tissue using methanol-facilitated solubilization and tryptic digestion coupled with 2D-LC-MS/MS. Nat. Protoc. *1*, 2784–2790.

Boyle, A.K., Rinaldi, S.F., Rossi, A.G., et al. (2018). Repurposing simvastatin as a therapy for preterm labor: evidence from preclinical models. FASEB J. *33*, 2743–2758.

Buhaescu, I., and Izzedine, H. (2007). Mevalonate pathway: a review of clinical and therapeutical implications. Clin. Biochem. *40*, 575–584.

Bulletti, C., De Ziegler, D., Setti, P.E.L., et al. (2004). The patterns of uterine contractility in normal menstruating women: from physiology to pathology. Ann. NY Acad. Sci. *1034*, 64–83.

Casey, P.J. (1992). Biochemistry of protein prenylation. J. Lipid Res. *33*, 1731–1740.

Chen, Z., Xu, N., Chong, D., et al. (2018). Geranylgeranyl pyrophosphate synthase facilitates the organization of cardiomyocytes during mid-gestation through modulating protein geranylgeranylation in mouse heart. Cardiovasc. Res. *114*, 965–978.

Diao, F., Jiang, C., Wang, X., et al. (2016). Alteration of protein prenylation promotes spermatogonial differentiation and exhausts spermatogonial stem cells in newborn mice. Sci. Rep. *6*, 28917.

Foley, A., Zou, Y., Dunford, J., et al. (2020). GGPS1 mutations cause muscular dystrophy/hearing loss/ovarian insufficiency syndrome. Ann. Neurol. *88*, 332–347.

Gan, Y., Wang, J., Coselli, J.S., et al. (2008). Synergistic induction of apoptosis by HMG-CoA reductase inhibitor and histone deacetylases inhibitor in HeLa cells. Biochem. Biophys. Res. Commun. *365*, 386–392.

Garfield, R.E., and Maner, W.L. (2007). Physiology and electrical activity of uterine contractions. Semin. Cell Dev. Biol. *18*, 289–295.

Goldstein, J.L., and Brown, M.S. (1990). Regulation of the mevalonate pathway. Nature *343*, 425–430.

Gonzalez, J.M., Pedroni, S.M.A., and Girardi, G. (2014). Statins prevent cervical remodeling, myometrial contractions and preterm labor through a mechanism that involves hemoxygenase-1 and complement inhibition. Mol. Hum. Reprod. *20*, 579–589.

Haraguchi, H., Hirota, Y., Saitofujita, T., et al. (2019). Mdm2–p53–SF1 pathway in ovarian granulosa cells directs ovulation and fertilization by conditioning oocyte quality. FASEB J. *33*, 2610–2620.

He, W., Peng, Y.J., Zhang, W.C., et al. (2008). Myosin light chain kinase is central to smooth muscle contraction and required for gastrointestinal motility in mice. Gastroenterology *135*, 610–620.

Jiang, C., Diao, F., Sang, Y., et al. (2017). GGPP-mediated protein geranylgeranylation in oocyte is essential for the establishment of oocyte-granulosa cell communication and primary-secondary follicle transition in mouse ovary. PLoS Genet. *13*, e1006535.

Jorgez, C.J., Klysik, M., Jamin, S.P., et al. (2004). Granulosa cell-specific inactivation of follistatin causes female fertility defects. Mol. Endocrinol. *18*, 953–967.

Kamal, S., Khan, M.A., Seth, A., et al. (2017). Beneficial effects of statins on the rates of hepatic fibrosis, hepatic decompensation, and mortality in chronic liver disease: a systematic review and meta-analysis. Am. J. Gastroenterol. *112*, 1495–1505.

Kunz, G., and Leyendecker, G. (2002). Uterine peristaltic activity during the menstrual cycle: characterization, regulation, function and dysfunction. Reprod. Biomed. Online *4*, 5–9.

Leichner, G., Avner, R., Harats, D., et al. (2011). Metabolically regulated endoplasmic reticulum-associated degradation of 3-hydroxy-3-methylglutaryl-CoA reductase: evidence for requirement of a geranylgeranylated protein. J. Biol. Chem. *286*, 32150–32161.

Liu, J., Jiang, S., Zhao, Y., et al. (2018). Geranylgeranyl diphosphate synthase (GGPPS) regulates non-alcoholic fatty liver disease (NAFLD)–fibrosis progression by determining hepatic glucose/fatty acid preference under high-fat diet conditions. J. Pathol. *246*, 277–288.

Moghadasian, M.H. (1999). Clinical pharmacology of 3-hydroxy-3-methylglutaryl coenzyme A reductase inhibitors. Life Sci. *65*, 1329–1337.

Moutinho, M., Nunes, M.J., and Rodrigues, E. (2017). The mevalonate pathway in neurons: it's not just about cholesterol. Exp. Cell Res. *360*, 55–60.

Mraiche, F., Cena, J., Das, D., et al. (2005). Effects of statins on vascular function of endothelin-1. Br. J. Pharmacol. *144*, 715–726.

Nasioudis, D., Doulaveris, G., and Kanninen, T.T. (2019). Dyslipidemia in pregnancy and maternal-fetal outcome. Minerva Ginecol. *71*, 155.

Nasu, K., Yuge, A., Tsuno, A., et al. (2009). Simvastatin inhibits the proliferation and the contractility of human endometriotic stromal cells: a promising agent for the treatment of endometriosis. Fertil. Steril. *92*, 2097–2099.

Ofori, B., Rey, E., and Berard, A. (2007). Risk of congenital anomalies in pregnant users of statin drugs. Br. J. Clin. Pharmacol. *64*, 496–509.

Panda, T., and Devi, V.A. (2004). Regulation and degradation of HMGCo-A reductase. Appl. Microbiol. Biotechnol. *66*, 143–152.

Pedroni, S.M.A., Gonzalez, J.M., Wade, J., et al. (2014). Complement inhibition and statins prevent fetal brain cortical abnormalities in a mouse model of preterm birth. Biochim. Biophys. Acta *1842*, 107–115.

Perezguerrero, C., Marquezmartin, A., Herrera, M.D., et al. (2005). Regulation of vascular tone from spontaneously hypertensive rats by the HMG-CoA reductase inhibitor, simvastatin. Pharmacology *74*, 209–215.

Petersen, E.E., Mitchell, A.A., Carey, J.C., et al. (2008). Maternal exposure to statins and risk for birth defects: a case-series approach. Am. J. Med. Genet. A *146*, 2701–2705.

Redecha, P., Franzke, C.W., Ruf, W., et al. (2008). Neutrophil activation by the tissue factor/Factor VIIa/PAR2 axis mediates fetal death in a mouse model of antiphospholipid syndrome. J. Clin. Invest. *118*, 3453–3461.

Redecha, P., Van Rooijen, N., Torry, D.S., et al. (2009). Pravastatin prevents miscarriages in mice: role of tissue factor in placental and fetal injury. Blood *113*, 4101–4109.

Schafer, W.R., and Rine, J. (1992). Protein prenylation: genes, enzymes, targets, and functions. Ann. Rev. Genet. *26*, 209–237.

Smith, R., Imtiaz, M.S., Banney, D., et al. (2015). Why the heart is like an orchestra and the uterus is like a soccer crowd. Am. J. Obstetr. Gynecol. *213*, 181–185.

Su, Y., Sugiura, K., Wigglesworth, K., et al. (2007). Oocyte regulation of metabolic cooperativity between mouse cumulus cells and oocytes: BMP15 and GDF9 control cholesterol biosynthesis in cumulus cells. Development *135*, 111–121.

Sugiura, K., Pendola, F.L., and Eppig, J.J. (2005). Oocyte control of metabolic cooperativity between oocytes and companion granulosa cells: energy metabolism. Dev. Biol. *279*, 20–30.

Wang, X.-X., Ying, P., Diao, F., et al. (2013). Altered protein prenylation in Sertoli cells is associated with adult infertility resulting from childhood mumps infection. J. Exp. Med. *210*, 1559–1574.

Word, R.A., Stull, J.T., Casey, M.L., et al. (1993). Contractile elements and myosin light chain phosphorylation in myometrial tissue from nonpregnant and pregnant women. J. Clin. Invest. *92*, 29–37.

Xu, N., Guan, S., Chen, Z., et al. (2015). The alteration of protein prenylation induces cardiomyocyte hypertrophy through Rheb–mTORC1 signalling and leads to chronic heart failure. J. Pathol. *235*, 672–685.

Yeh, Y., Goto, T., Takahashi, N., et al. (2016). Geranylgeranyl pyrophosphate performs as an endogenous regulator of adipocyte function via suppressing the LXR pathway. Biochem. Biophys. Res. Commun. *478*, 1317–1322.